

# TEMPERATURE DEPENDENCE OF MASS PARAMETERS AND FISSION BARRIERS\*

A. BARAN AND Z. ŁOJEWSKI

Institute of Physics, Maria Curie-Skłodowska University  
pl. M. Curie-Skłodowskiej 1, 20-031 Lublin, Poland

(Received March 14, 1994; revised version received May 16, 1994)

In the unified temperature dependent nuclear model with Woods-Saxon single particle potential the adiabatic mass parameters and potential energies are calculated and discussed. Both liquid drop and shell correction are temperature dependent. Shell structure of mass parameter and fission barriers vanish for hot nuclear systems at  $T = 1.5$  MeV. The mass parameter is shown to have irrotational behaviour at high temperature.

PACS numbers: 24.75.+i, 25.85.Ca

## 1. Introduction

The fundamental quantity which enters the fission dynamics and fission half-lives is the mass tensor (mass parameter)  $B_{kl}(\beta)$ . It is a function of deformations ( $\beta$ ).

In considering heavy ion reactions or pre/post collision fission, one is dealt with a sort of intrinsic excitations and it is highly desirable to investigate the collective motion of the nucleus-like system at this specific finite excitation energy, *i.e.* finite temperature.

The first papers on temperature dependence of fission barriers were done in seventies by Jensen and Damgaard [1].

Diebel, Albrecht and Hasse [2] presented the extended temperature dependent calculations of energy and the moment of inertia. In that paper the temperature dependence of the liquid drop model was used and discussed in the case of heavy nuclei.

The review of nuclear fission barriers is given in the paper by Łojewski, Pashkevich and Ćwiok [3] for various temperatures. The authors have used the cold liquid drop model and temperature dependent shell correction.

---

\* This research is partly supported by the KBN grant No 2 0312 91 01.

One of the first papers on temperature dependence of mass parameters were published by Iwamoto and Greiner [4] and Iwamoto and Maruhn [5]. The authors show the qualitative estimates of mass parameters in the harmonic oscillator potential and with the Fermi gas model. According to these papers, the mass parameter increases with temperature.

In a paper by Schneider, Maruhn and Greiner [6] it is shown the singular behaviour of the mass parameter at the critical temperatures. They pointed out that the mass decreases in the case of more realistic nuclear model.

The purpose of this paper is to investigate the behaviour of mass parameter and fission barriers on temperature as well as deformation. The present paper unifies the temperature dependence of the nuclear collective hamiltonian and shows the calculations of both potential energy barriers and the mass parameters as a functions of deformation and temperature using the realistic Woods–Saxon single particle potential with the “universal” set of parameters [7]. We improve the irrational behaviour of the mass parameter in the vicinity of the critical temperature by means of smoothing the level densities at the level crossings.

It is shown that the mass parameter decreases to its irrotational value with increasing temperature. Fission barriers at low temperatures show the known shell structure which washes out at temperatures  $T > 1$  MeV.

In the following two sections we show the basic BCS equations and mass parameters derived in the adiabatic cranking approximation. The next two sections are devoted to temperature dependent calculations of hot nuclear liquid drop and fission barriers. The results of the calculations are presented in Section 6.

## 2. Temperature dependent BCS model

In order to introduce thermal excitations, we employ the grand canonical formalism. The grand potential function  $\Omega$  for the one type of nucleons may be expressed as follows [1]

$$\Omega = -T \ln \mathcal{Z} = \sum_{k>0} (\epsilon_k - \lambda - E_k) - 2T \sum_{k>0} \ln \left[ 1 + \exp \left( -\frac{E_k}{T} \right) \right] + \frac{\Delta^2}{G}. \quad (1)$$

Here  $\mathcal{Z}$  is the grand partition function and the quasiparticle energy  $E_k$  is  $E_k = [(\epsilon_k - \lambda)^2 + \Delta^2]^{1/2}$ . In the whole paper the temperature  $T$  is expressed in MeV and is defined according to Bohr and Mottelson [8]. The gap parameter  $\Delta(T)$  and the chemical potential  $\lambda(T)$  are determined by the coupled gap- and particle number equations:

$$\frac{2}{G} = \sum_{k>0} \frac{1}{E_k} \tanh \frac{E_k}{2T}, \quad (2)$$

$$N = \sum_{k>0} \left( 1 - \frac{\epsilon_k - \lambda}{E_k} \tanh \frac{E_k}{2T} \right). \quad (3)$$

The usual BCS equations can be obtained from the above formulae in the limit of zero temperature,  $T \rightarrow 0$ .

At finite  $G$ , the gap  $\Delta(T)$  is an decreasing function of the temperature. It decreases monotonically until the pairing correlations completely vanish. It happens at critical temperature  $T_c$  which for typical situations is shown to be close to 0.5 MeV.

### 3. Mass parameter

We start with the classical microscopic Hamiltonian of the form

$$\mathcal{H} = H_s + H_{\text{pair}}, \quad (4)$$

where

$$H_s = \sum_{\mu} (\epsilon_{\mu} - \lambda) (a_{\mu}^{\dagger} a_{\mu} + a_{\bar{\mu}}^{\dagger} a_{\bar{\mu}}) \quad \text{and} \quad H_{\text{pair}} = -G \sum_{\mu\nu} a_{\mu}^{\dagger} a_{\bar{\mu}}^{\dagger} a_{\bar{\nu}} a_{\nu}, \quad (5)$$

and  $a_{\mu}^{\dagger}$ ,  $a_{\mu}$  are particle creation and annihilation operators in the state  $\mu$ . The state  $\bar{\mu}$  denotes the time reversed state to that of  $\mu$ .

In calculations we use pairing strength constants as follows. For protons  $G_Z A = 13.3 + 0.217(N - Z)$  and for neutrons  $G_N A = 19.3 - 0.084(N - Z)$  [9].  $N$ ,  $Z$  and  $A$  are proton, neutron and mass number  $A = N + Z$  respectively. The number of levels in the pairing window equals to the number of particles ( $Z$  or  $N$ ) and is counted from the bottom of the energy spectrum.

In the adiabatic cranking model the collective mass  $B_{kl}(\hat{\beta})$  reads [10]

$$B_{kl}(\hat{\beta}) = 2\hbar^2 \sum_{m \neq 0} \frac{\langle m | \frac{\partial \mathcal{H}}{\partial \beta_k} | 0 \rangle \langle 0 | \frac{\partial \mathcal{H}}{\partial \beta_l} | m \rangle}{(\epsilon_m - \epsilon_0)^3}, \quad (6)$$

where  $|m\rangle$  and  $|0\rangle$  denote the wave function of the excited and ground state of the nucleus respectively,  $\epsilon_m$  and  $\epsilon_0$  are the corresponding single particle energies and  $\hat{\beta}$  is a set of deformation variables.

After transforming to the quasi-particle representation, the derivative of the Hamiltonian over the deformation, takes the following form

$$\begin{aligned} \frac{\partial \mathcal{H}}{\partial \beta_k} = & \sum_{\mu \neq \nu} \langle \mu | \frac{\partial H_s}{\partial \beta_k} | \nu \rangle \\ & \times \left\{ (u_{\mu} u_{\nu} - v_{\mu} v_{\nu}) (\alpha_{\mu}^{\dagger} \alpha_{\nu} + \alpha_{\bar{\mu}}^{\dagger} \alpha_{\bar{\nu}}) + (u_{\mu} v_{\nu} + v_{\mu} u_{\nu}) (\alpha_{\mu}^{\dagger} \alpha_{\bar{\nu}}^{\dagger} - \alpha_{\bar{\mu}} \alpha_{\nu}) \right\} \\ & + \sum_{\mu} \left( \frac{\Delta}{E_{\mu}} \frac{\partial}{\partial \beta_k} (\epsilon_{\mu} - \lambda) - \frac{\epsilon_{\mu} - \lambda}{E_{\mu}} \frac{\partial \Delta}{\partial \beta_k} \right), \end{aligned} \quad (7)$$

here  $|\mu\rangle$  and  $|\nu\rangle$  are the single particle (Woods-Saxon potential) eigenstates and  $v_\mu$ ,  $u_\mu$  are the pairing probability factors. The  $H_s$  is the single particle Hamiltonian.

After some algebra, the final results can be brought into the form

$$B_{kl}(\hat{\beta}) = B_{kl}^{(1)}(\hat{\beta}) + B_{kl}^{(2)}(\hat{\beta}) + B_{kl}^{(3)}(\hat{\beta}). \quad (8)$$

The selected parts are the following

$$B_{kl}^{(1)}(\hat{\beta}) = \hbar^2 \sum_{\mu\nu} \langle \mu | \frac{\partial H_s}{\partial \beta_k} | \nu \rangle \langle \nu | \frac{\partial H_s}{\partial \beta_l} | \mu \rangle \times \frac{(u_\mu v_\nu + v_\mu u_\nu)^2}{(E_\mu + E_\nu)^3} \left( \tanh \left( \frac{E_\mu}{2kT} \right) + \tanh \left( \frac{E_\nu}{2kT} \right) \right), \quad (9)$$

$$B_{kl}^{(2)}(\hat{\beta}) = \hbar^2 \sum_{\mu \neq \nu} \langle \mu | \frac{\partial H_s}{\partial \beta_k} | \nu \rangle \langle \nu | \frac{\partial H_s}{\partial \beta_l} | \mu \rangle \times \frac{(u_\mu u_\nu - v_\mu v_\nu)^2}{(E_\mu - E_\nu)^3} \left( \tanh \left( \frac{E_\mu}{2kT} \right) - \tanh \left( \frac{E_\nu}{2kT} \right) \right), \quad (10)$$

$$B_{kl}^{(3)}(\hat{\beta}) = \hbar^2 \sum_{\mu} \frac{1}{4E_\mu^5} \tanh \left( \frac{E_\mu}{2kT} \right) \left\{ -2\Delta \langle \mu | \frac{\partial H_s}{\partial \beta_k} | \mu \rangle \left[ \Delta \frac{\partial \lambda}{\partial \beta_l} + (\varepsilon_\mu - \lambda) \frac{\partial \Delta}{\partial \beta_l} \right] + \left( \Delta \frac{\partial \lambda}{\partial \beta_k} + (\varepsilon_\mu - \lambda) \frac{\partial \Delta}{\partial \beta_k} \right) \left( \Delta \frac{\partial \lambda}{\partial \beta_l} + (\varepsilon_\mu - \lambda) \frac{\partial \Delta}{\partial \beta_l} \right) \right\}. \quad (11)$$

This formula coincides with the usual expression in the limit of zero temperature.

As we shall show in Section 4 such a division of mass parameter into three components is convenient in analysis of its temperature dependence. We shall analyze the behaviour of mass in the wide range of the nuclear temperatures and the broad class of nuclei.

#### 4. Heated liquid drop model

For the macroscopic part of energy we employ the  $T$ -dependent liquid drop model based on the results of the Thomas-Fermi description of the excited nucleus [10].

The following expression for the nuclear density  $n(T)$  and the nuclear surface tension  $\sigma(T)$  were adapted from Ref. [2]

$$n(T) = n(0) [1 - \alpha T^2], \quad \alpha = 0.0032 \text{ MeV}, \quad (12)$$

$$\sigma(T) = \sigma(0) [1 - \gamma T^2], \quad \gamma = 0.0114 \text{ MeV}. \quad (13)$$

The free deformation energy, normalized to zero for spherical shape can be written as

$$F^{\text{LD}}(\hat{\beta}, T) = E_{\text{surf}}(\hat{\beta}, T = 0) [1 - (\gamma - 2\alpha/3)T^2] + E_{\text{coul}}(\hat{\beta}, T = 0) [1 - \alpha T^2/3]. \quad (14)$$

The entropy  $S$  and energy  $E$  may be obtained from the following thermodynamical relations

$$S = -\frac{\partial F}{\partial T}, \quad (15)$$

$$E = F + TS. \quad (16)$$

Finally, the macroscopic part of energy is given by

$$E^{\text{LD}}(\hat{\beta}, T) = (B_s - 1)E_{\text{surf}}(\text{sphere, cold}) \left[1 + \left(\gamma - 2\frac{\alpha}{3}\right)T^2\right] + (B_c - 1)E_{\text{coul}}(\text{sphere, cold}) \left[1 + \frac{\alpha T^2}{3}\right], \quad (17)$$

where the usual surface and Coulomb energies are denoted by  $E_{\text{surf}}(\text{sphere, cold})$  and  $E_{\text{coul}}(\text{sphere, cold})$  respectively and  $B_s$  and  $B_c$  are the ratios of the corresponding nuclear energies at finite deformations to this values, *e.g.*,  $B_s = E_{\text{surf}}(\hat{\beta}, T)/E_{\text{surf}}(0, 0)$ .

## 5. Fission barriers

We use an extended version of the Strutinsky macro-microscopic method to calculate an effective potential barriers for internally excited ( $T > 0$ ) nuclei. The internal energy of the hot nucleus is written as

$$E(\hat{\beta}, T) = E^{\text{LDM}}(\hat{\beta}, T) + \delta E(\hat{\beta}, T). \quad (18)$$

The first term is the average energy of a heated liquid drop. Strutinsky shell correction, including temperature dependent pairing is a second term.

Following Ref. [2] we define the shell-plus-pairing corrections to the energy for  $T \geq 0$  and for the one type of nucleons as

$$\delta E(\hat{\beta}, T) = E^{\text{BCS}}(\hat{\beta}, T) - \bar{E}^{\text{BCS}}(\hat{\beta}, T), \quad (19)$$

where  $E^{\text{BCS}}$  is the energy of the hot nucleus calculated in the temperature dependent BCS picture. The second term gives the smooth energy evaluated in Strutinsky procedure. Some details of the method are described in [2].

The free energy is obtained from the thermodynamic relation

$$F = E - TS, \quad (20)$$

in which  $S$  is the entropy of the nucleus.

The way of statistical description of excited nuclei depends on the process one considers:

- The nuclear fission may be treated as an isothermal thermodynamical process. In this case the free energy  $F(\hat{\beta}, T)$  is the associated effective potential rather than the internal energy [8]  $E(\hat{\beta}, T)$ , which has often been used in the literature.
- In the adiabatic limit, however, the isentropic processes at  $S = \text{const}$  are to be more realistic. In this case the  $E(\hat{\beta}, T(S))$  is the associated effective thermodynamical potential.

Since usually only the deformation dependent parts of the potentials are of interest, we note that both  $F$  and  $E$  are equivalent with this respect only if  $S$  does not depend on deformation [3]. In general this condition is not fulfilled. However, at large temperature, the entropy changes only a little with deformation.

## 6. Results

We begin the discussion of results starting from Eqs (9), (10), (11) for the components  $B_{kl}^{(1)}$ ,  $B_{kl}^{(2)}$  and  $B_{kl}^{(3)}$  of mass parameter  $B_{kl}$ . This parts of mass were naturally selected to show their specific behaviour under the change of temperature and deformation.

The very important consequences on the behaviour of nucleus come from the existence in the system the critical temperature  $T_c$  at which pairing correlations disappear. In fact there are two critical temperatures one for each isospin component. For the nucleus  $^{250}\text{Fm}$  which was chosen for illustration this corresponds approximately to 0.4 MeV and 0.6 MeV for protons and neutrons respectively. The vanishing of the pairing gap  $\Delta$  at the temperature  $T = T_c$  is the outcome of the adapted simple standard pairing model. This is not the case in a more sophisticated models of residual interactions which include the particle number projection, *e.g.*, Esebbag and Egido [12].

In the following we shall consider the nucleus  $^{250}\text{Fm}$ . The subscripts  $k$  and  $l$  refer to deformation parameter  $\beta_2$ . All other deformation parameters are set equal to zero. The discussion of the mass parameter behaviour as a function of the temperature is done for deformation  $\beta_2 = 0.2$  which corresponds approximately to the equilibrium of the nucleus at all considered temperatures.

The singularities shown by the nuclear mass parameters are due to the single particle level crossings [13, 14]. We have done the careful analysis of each of three parts separately in order to find the term in formula (8) responsible for the singularity.

Fig. 1 represents the part  $B_{kl}^{(1)}$  Eq. (9) of mass parameter *vs* temperature separately for protons (thin line) and neutrons (thick line) as well as the total  $B_{kl}^{(1)}$  part of mass (very thick line). At the critical temperature  $T_c$  one sees characteristic increase of each isospin component of the mass with temperature. After reaching  $T_c$  both neutron and proton components of  $B_{kl}^{(1)}$  decrease asymptotically.

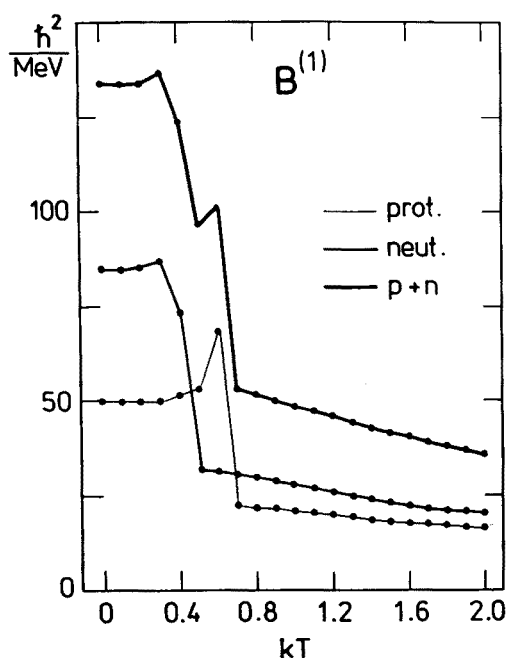


Fig. 1. The part  $B_{kl}^{(1)}$  of mass parameter *vs* temperature. Protons are represented by thin line, neutrons by thick line and the total  $B_{kl}^{(1)}$  part of mass by very thick line.

The most regular is the second part of mass parameter denoted by  $B_{kl}^{(2)}$  Eq. (10). It is displayed in Fig. 2. The same convention is used as before. It is interesting to note the smallness of this part of the mass tensor under the critical temperature. It is absent practically up to temperatures from the vicinity of  $T_c$ . Then we can observe very regular increase of the proton and as well as the total part of  $B_{kl}^{(2)}$ . It saturates for temperatures  $T > 2$

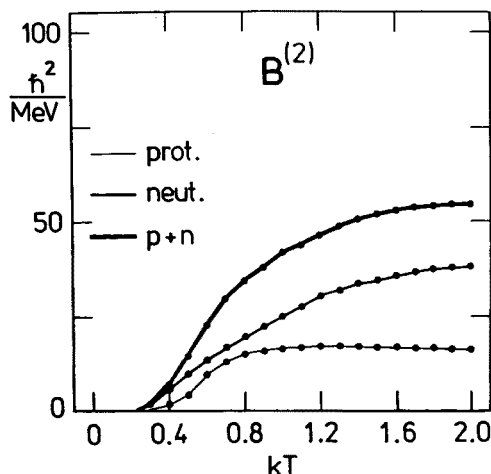


Fig. 2. The same as Fig. 1 but for  $B_{kl}^{(2)}$  part of mass parameter.

MeV. Here we have used the smoothing procedure for level densities which will be described.

An important feature of the mass parameter can be studied in Figs 3 and 4 together. Fig. 3 shows the third "singular" component of the mass  $B_{kl}^{(3)}$  Eq. (11). The singularity as expected appears at critical temperatures: for protons at  $T = 0.4$  MeV and neutrons at  $T = 0.6$  MeV. This singular behaviour at critical temperatures can be seen also in Fig. 4 where the whole mass parameter Eq. (8) is drawn. In the temperature range between both  $T_c$  points, the mass parameter is not well defined. It is rapidly changing function of  $T$ . At  $(T - T_c) \rightarrow 0$ , parameter  $B_{kl} \rightarrow \infty$ . For temperature  $T > T_c$  this term of mass parameter disappears. This is the result of zero pairing gap parameter (see Eq. (11)) in this range of temperature.

The mechanism of such behaviour is the following. At the critical temperature  $T_c$  the pairing gap vanishes. Taking this into account one expects intensive energy level crossings at each deformation. It leads to decreasing the energy denominators in Eqs (9)–(11) which are not compensated by the similar nominators. As the consequence this part of mass parameters unphysically explodes. This behaviour was already observed in the case of the simple harmonic oscillator model [4, 5]. At the same time the second part of the mass parameter is finite after elimination of the level crossings. The same is to be said about  $B_{kl}^{(1)}$ , which has no singularities at all.

There is no real physical reason for singular behaviour of nuclear mass parameter with temperature. Therefore, in the calculations we applied the solution to this problem based on the assumption of nondegenerate energy spectrum of nuclear system. Taking it as a rule we assume that the en-



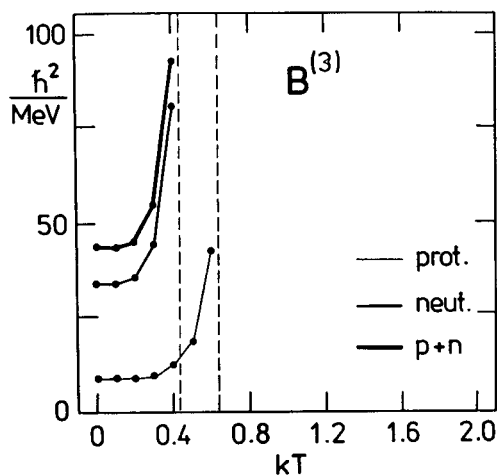


Fig. 3. The same as Fig. 1 but for  $B_{kl}^{(3)}$  part of mass parameter. The vertical dashed lines mark protons and neutrons critical temperatures.

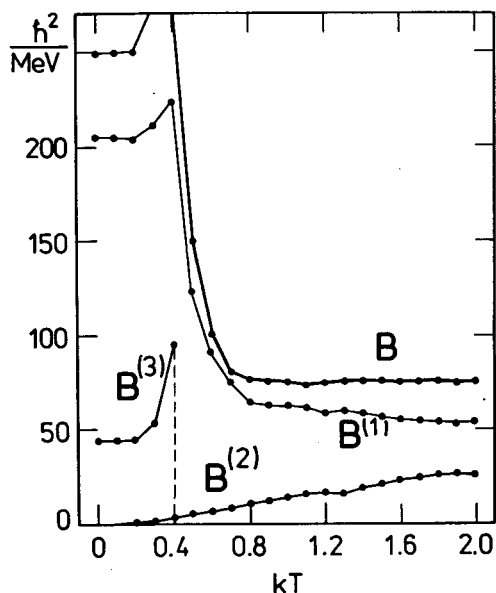


Fig. 4. Total mass parameter  $B_{kl}$  and its three parts as functions of temperature. Deformation  $\beta_2 = 0.2$ .

ergy levels are nondegenerate at any deformation. Calculating the energy level density  $\rho(\beta, T)$  (from the quasi-particle spectrum, which is equal to the particle-hole excitation density at the critical temperature) one has the average local distance of levels  $\delta = 1/\rho(\beta, T)$ . This distance may be used in

calculations of "singular" parts of mass parameter.

We applied this procedure and have overcome all difficulties with unphysical singularities which are the consequences of the poor model for the mass parameter. We want to stress here that the same model behaves well and gives good results in other situations of interest (see spontaneous fission half lives calculated with it [15]).

After the loss of pairing correlations the nuclear mass tends to its irrational value [15]. In the spherical case the latter is given by the formula

$$B_{\text{irr}} = \frac{2}{15} AMR_0^2, \quad (21)$$

where  $A$ ,  $M$  and  $R_0$  are mass number, nucleon mass and average nuclear radius respectively. In the case of  $^{250}\text{Fm}$  it is approximately  $50\hbar\text{MeV}^{-1}$ . We interpret this fact as the loss of collectivity of the nucleus at high temperature.

The above conclusion contradicts the results of paper [5] where the mass parameter was estimated to increase with the temperature up to its adiabatic value.

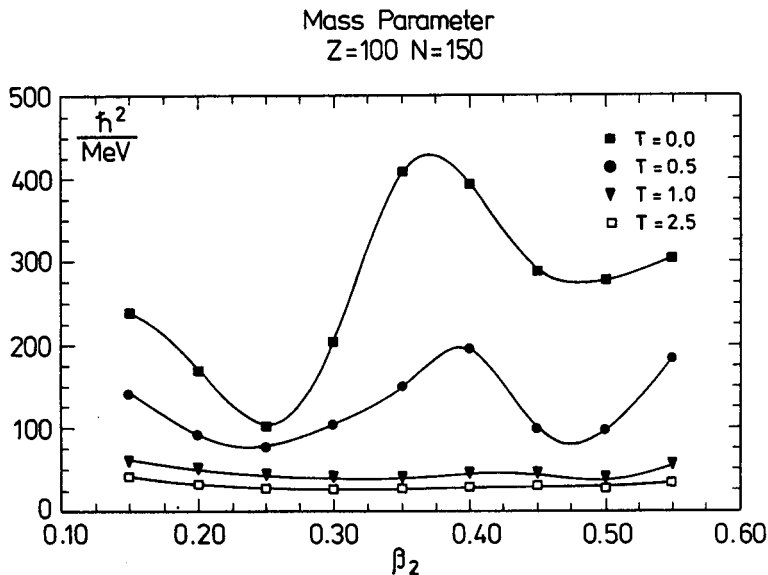


Fig. 5. Total mass parameter as a function of deformation for diverse temperatures.

The whole mass parameter of  $^{250}\text{Fm}$  as a function of deformation at various temperatures is shown in Fig. 5. The temperature changes from 0 MeV (the most upper curve) to 2.5 MeV (the lowest curve). The upper limit (lowest curve) corresponds to  $E^* \approx 40$  MeV excitation energy. One sees that the shell effects are completely washed out at temperatures  $T > 1.5$

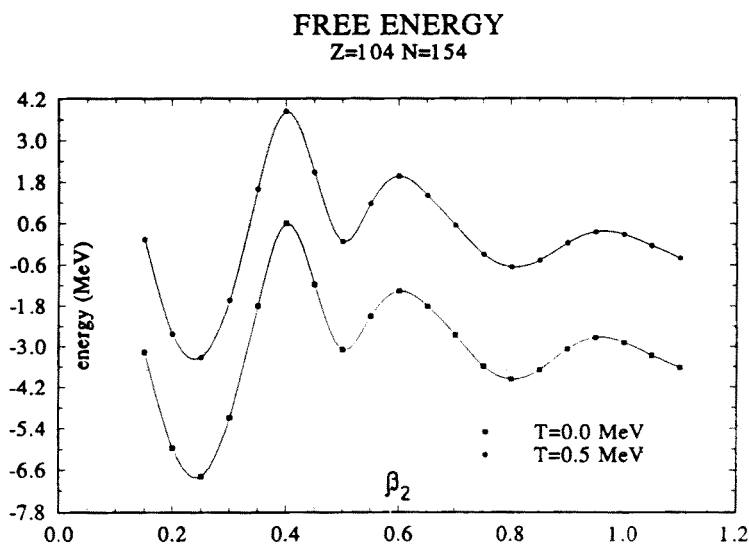


Fig. 6a. Free energy vs deformation for  $T = 0$  MeV (upper curve) and  $T = 0.5$  MeV of  $^{258}_{104}$ .

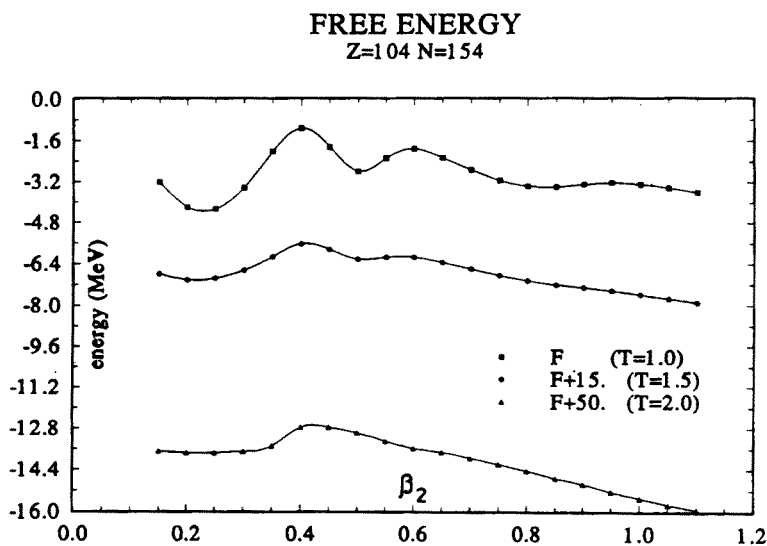


Fig. 6b. Free energy vs deformation for  $T = 1$  MeV (upper curve),  $T = 1.5$  MeV and  $T = 2$  MeV of  $^{258}_{104}$ .

MeV. The mass parameter of the hot nucleus does not depend on deformation and as it was already said it reaches its irrotational limit Eq. (21). It means that the long range nuclear correlations are also lost. The nucleus behaves like irrotational liquid. At lower temperatures the shell structure is present. In Figs 6a and 6b we show the whole fission barriers (free energy) for the nucleus  $^{258}104$ . The shell structure present at low temperatures disappears at temperatures higher then 1.5 MeV (lower curve in Fig. 6b). This result has been observed before [3].

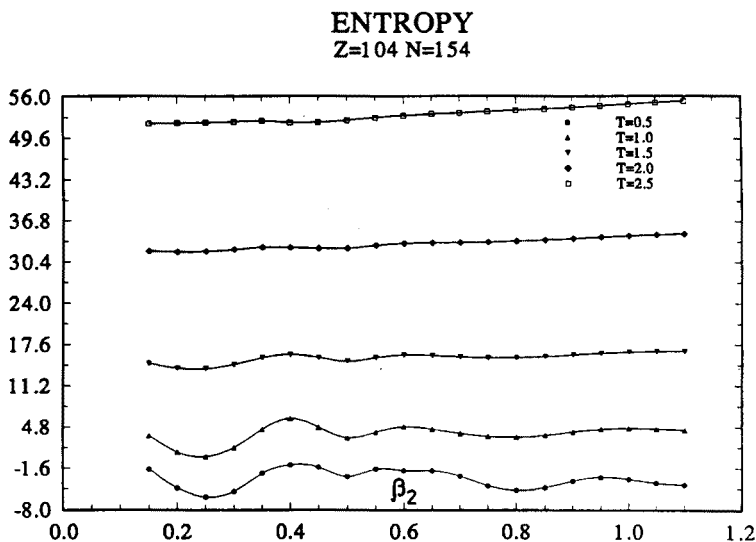


Fig. 7. Entropy of the nucleus  $^{258}104$  at different temperatures.

It is interesting to see other characteristics of the nucleus as a function of temperature. Let us look at the entropy of the  $^{258}104$ . It is shown in Fig. 7. As one expects the entropy increases with the temperature and shows the similar shell effects as the free energy and mass parameter.

The effect of the critical temperature is not seen in free energy and the entropy behaviour.

The only quantity with consequences coming from the existence of critical temperatures is the mass parameter.

At the end of this presentation we show two other figures in which average behaviour (liquid drop model) of the free energy (Fig. 8) and energy (Fig. 9) is shown. The temperature lowers the liquid drop fission barriers for both free energy and the energy.

The above analysis shows that the mass parameter and the free energy barriers are very sensitive functions of the temperature. It is important to know its dependence and the mechanisms behind in all situations in

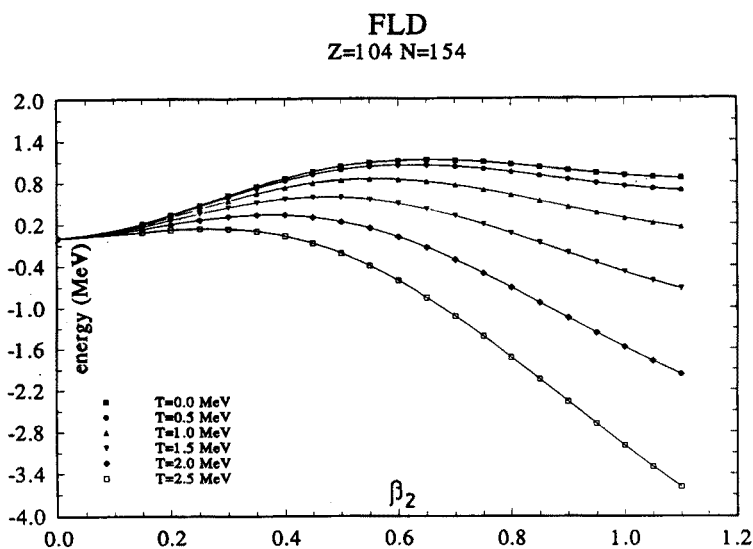


Fig. 8. Free energy  $F$  of the liquid drop nucleus  $^{258}_{104}$ .

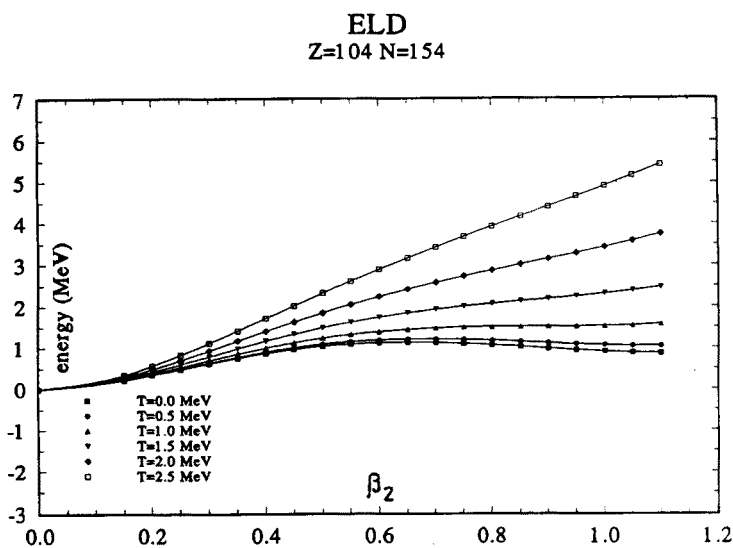


Fig. 9. Internal energy  $E$  of the liquid drop nucleus  $^{258}_{104}$ .

which one studies the hot nuclear systems. This are typically the heavy ion collision processes and the fragmentation of the excited nuclei.

We are thankful to Professor Krzysztof Pomorski for very valuable comments and critical reading of the manuscript.

## REFERENCES

- [1] A.S. Jensen, J. Damgaard, *Nucl. Phys.* **A232**, 578 (1973).
- [2] M. Diebel, K. Albrecht, R. Hasse, *Nucl. Phys.* **A355**, 66 (1981).
- [3] Z. Łojewski, V.V. Pashkevich, S. Ćwiok, *Nucl. Phys.* **A436**, 499 (1985).
- [4] A. Iwamoto, W. Greiner, *Z. Phys.* **A292**, 301 (1979).
- [5] A. Iwamoto, J.A. Maruhn, *Z. Phys.* **A293**, 315 (1979).
- [6] V. Schneider, J. Maruhn, W. Greiner, *Z. Phys.* **A323** 111 (1986).
- [7] S. Ćwiok *et al.*, *Comput. Phys. Commun.* **46**, 379 (1987).
- [8] A. Bohr, B. Mottelson, *Nuclear Structure*, vol. I, Benjamin, Amsterdam 1969.
- [9] J. Dudek, A. Majhofer, J. Skalski, *J. Phys. G* **6**, 447 (1980).
- [10] L. Wilets, *Theories of Nuclear Fission*, Clarendon Press, Oxford 1964.
- [11] R.W. Hasse, W. Stöcker, *Phys. Lett.* **44B**, 26 (1973).
- [12] C. Esebbag, J.L. Egido, *Nucl. Phys.* **A552**, 205 (1993).
- [13] Z. Łojewski, A. Góźdź, *Phys. Lett.* **B213**, 107 (1988).
- [14] F.A. Ivaniuk, *Z. Phys.* **A334**, 69 (1989).
- [15] S.G. Nilsson, C.F. Tsang, A. Sobiczewski, Z. Szymański, S. Wycech, C. Gustafson, I.L. Lamm, P. Möller, B. Nilsson, *Nucl. Phys.* **A131**, 1 (1969).